Electronic Supplementary Material (ESI) for Nanoscale.

Supporting information

Field enhancement of MoS_2: visualization of enhancement and effect of the number of layers

Masanori Sakamoto[a], Ken-ichi Saitow[a, b*]

[a]Department of chemistry, Graduate school of science, Hiroshima University,

1-3-1 Kagamiyama, Higashi Hiroshima, Hiroshima 739 8526, JAPAN.

[b]Natural science center for Basic R&D (N-BARD), Hiroshima University,

1-3-1 Kagamiyama, Higashi Hiroshima, Hiroshima 739 8526, JAPAN.

*Corresponding author

K.S. (telephone & fax: +81-82-424-7487, email: saitow@hiroshima-u.ac.jp)

Table S1 Reported thicknesses of MoS_2 monolayer using four preparation methods

Thickness of monolayer (nm)	Procedures	References
1.9	sonication[a]	*Nat Commun.*, 2014, **5**, 4576.
1.5		*J. Phys. Chem*. C., 2017, **121**, 4747 – 4759
1.2		*Nano Lett.*, 2015, **15**, 5449–5454.
0.9-1.2		*Angew. Chem. Int. Ed.*, 2011, **50**, 10839 –10842
1.2		*Chem. Mater.,* 2018, **30**, 5593 – 5601
0.9-1.2		*Science*, 2011, **331**, 568–571
1.1		*Acs Appl Mater Inter.*, 2014,**6**, 7084–7089
0.7		*Chem. Mater.*, 2015, **27**, 53 – 59
0.65-0.7	mechanical[b]	*Acs Nano*, 2011, **5**, 7707–7712.
0.65		*Nature Nanotechnology*, 2011, **6**, 147–150.
0.6-0.7		*Acs Nano*, 2010, **4**, 2695–2700.
0.8		*small*, 2012, **8**, No. 1, 63–67
0.53		*Nano Lett.*, 2011, **11**, 5148–5153.
0.65-0.8		*Nano Lett*., 2013, **13**, 668 – 673
0.54		*Appl Phys Lett.*, 2010, **96**, 213116.
0.7		*Nano Lett.*, 2010, **10**, 1271–1275
0.8		*ACS Nano*, 2012, **6** , 74–80
1-1.2	chemical[c]	*Nano Lett.*, 2011, **11**, 5111–5116
1.2-1.4		*ACS Omega,* 2017, **2**, 4678 – 4687
1.6		*Angew. Chem.,* 2013, **125**, 4254 –4258
1.0		*Angew. Chem. Int. Ed.*, 2011, **50**, 11093 –11097
~1.5		*J. Am. Chem. Soc.*, 2013, **135**, 4584 – 4587
0.72	CVD[d]	*Adv Mater.*, 2012, **24**, 2320–2325
0.7		*Nature Materials*, 2013, **12**, 754–759
0.65		*Nanoscale*, 2017, **9**, 2541–2547.
0.7		*Nano Lett.,* 2016, **16**, 1097 – 1103
0.7		*ACS Appl. Mater. Interfaces.,* 2017, **9**, 12073 – 12081
0.56		*ACS nano*, 2014, **8**, 10551-10558
0.8		*Nano Lett*., 2015, **15**, 198 – 205
0.7		*Acs Nano*, 2016, **10**, 1067–1075.

[a] Exfoliation by a sonication method in a solvent. [b] Exfoliation by the scotch tape. [c] Exfoliation by a lithium intercalation method, e.g. butyllithium. This method may cause phase transition to a metastable phase where the coordination of Mo atoms becomes octahedral , and the structure has metallic characteristic. [d] Synthesis from chemical vapor deposition (CVD) method

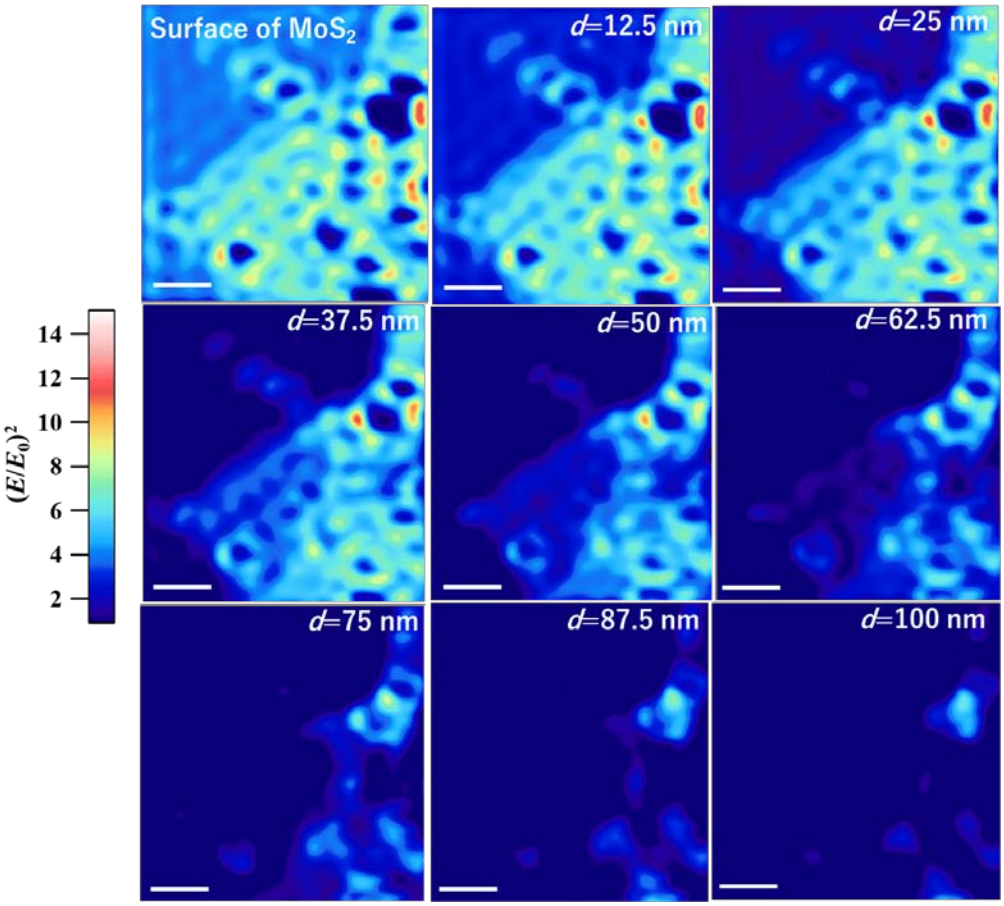

Fig. S1 EF mappings of electric fields obtained from FDTD calculations of a MoS_2 flake, whose *x*-*y*-*z*-positions are determined from AFM measurement. The calculations are conducted as a function of the depth of the MoS_2 flake, i.e. from the surface at $d = 0$ to the depth of $d = 100$ nm at the interval of 12.5 nm. The summation of the above nine calculated results gives Fig.4a. The scale bars denote 1μm. E and E_0 represent the magnitudes of electric fields with MoS_2 and without MoS_2, respectively.

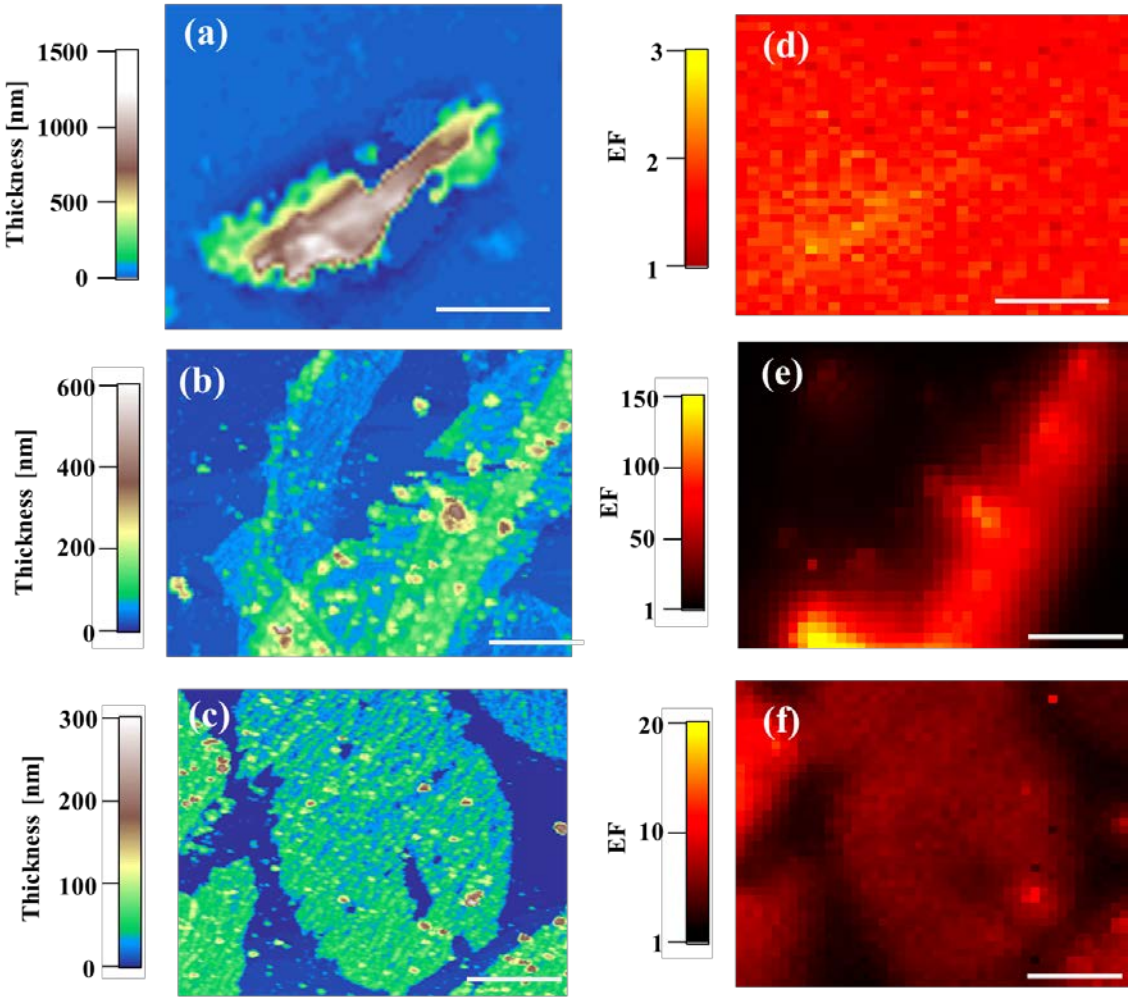

Fig. S2 (a) Laser microscope image of MoS_2 flakes. (b)(c) AFM images of MoS_2 flakes. (d)–(f) EF mappings are obtained from enhanced fluorescence intensities of CV using MoS_2 flakes at the same surfaces of the MoS_2 flakes in Fig. 2a–2c respectively. The bars denote the length of 5 μm. As for the grid sizes, the data of laser microscope, AFM and fluorescence micro spectroscopy images are set as 250 nm, 100 nm, and 500 nm, respectively.

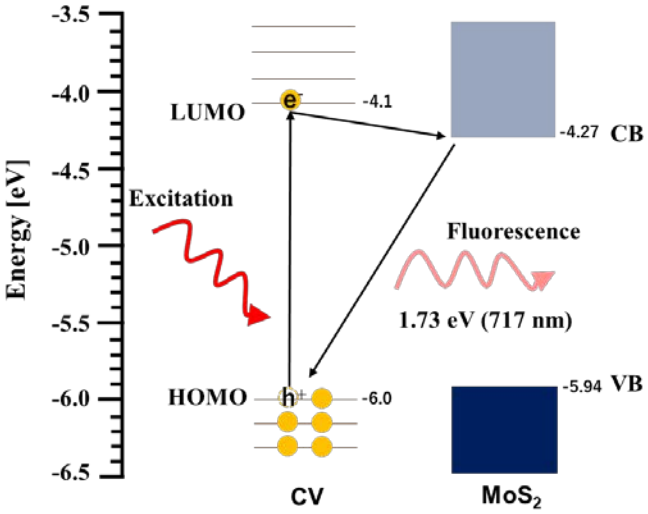

Fig. S3 Schematic diagram of a charge transfer (CT) band observed at around 720 nm in Fig. 8c. Black lines and navy rectangular represent electronic states of a crystal violet (CV) molecule and the band structure of bulk MoS_2, respectively. The former and latter energy levels are used as the data in ref. 1 and refs. 2 and 3, respectively; the highest occupied molecular orbital (HOMO), the lowest occupied molecular orbital (LUMO), conduction band (CB), and valence band (VB). The black arrows denote an optical transition of an electron of CV and recombination process between electron and hole via a CT process.

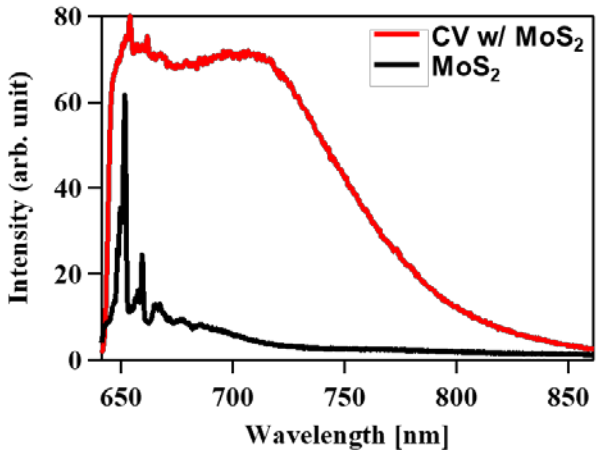

Fig. S4 Luminescence spectra measured with a MoS_2 (ca.800 layers) flake at an excitation wavelength of 632.8 nm. Red and black curves denote the fluorescence spectrum of CV solution without MoS_2 and photoluminescence & Raman spectra of MoS_2, respectively.

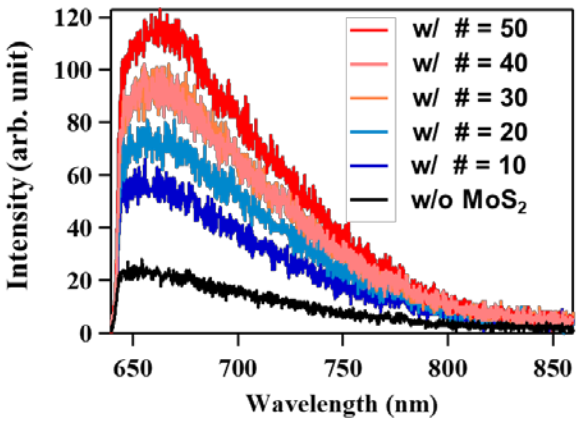

Fig. S5 Fluorescence spectra of CV solution with MoS_2 ranging from the number of layers (#) =10 to 50 (color curves). Fluorescence spectrum of CV solution without MoS_2 (black curve).

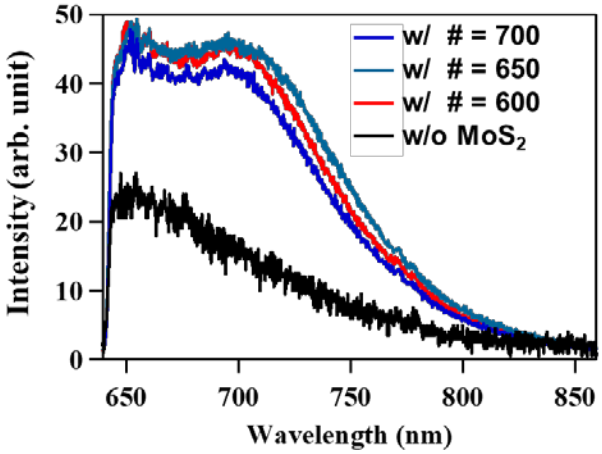

Fig. S6 Fluorescence spectra of CV solution with MoS_2 ranging from the number of layers (#) = 600 to 700 (color curves). Fluorescence spectrum of CV solution without MoS_2 (black curve).

Calculation of the extinction efficiency (Q_{ext})

We obtained the extinction efficiency (Q_{ext}) of MoS_2 using the Mie theory[5], based on the following equations. Q_{ext} is expressed by $Q_{ext} = Q_{abs} + Q_{sca,}$, where Q_{abs} is absorption efficiency and Q_{sca} the scattering efficiency. The Q_{ext} and Q_{sca} components are formulated as follows:

$$Q_{\text{ext}} = \frac{2}{x^2}\sum_{N=1}^{\infty}(2N+1)\text{Re}[a_N + b_N], \quad \text{(S1)}$$

$$Q_{\text{sca}} = \frac{2}{x^2}\sum_{N=1}^{\infty}(2N+1)[|a_N|^2 + |b_N|^2], \quad \text{(S2)}$$

where N is an integer, i.e. N=1, 2, and 3 correspond to electro and magnetic dipole, quadrupole, and hexapole modes, respectively. a_N (electric component) and b_N (magnetic component) are expressed as follows:

$$a_N = \frac{m\ \Psi_N(mx)\Psi'_N(x) - \Psi_N(x)\Psi'_N(mx)}{m\Psi_N(mx)\xi'_N(x) - \xi_N(x)\Psi'_N(mx)}, \quad \text{(S3)}$$

$$b_N = \frac{\Psi_N(mx)\Psi'_N(x) - m\Psi_N(x)\Psi'_N(mx)}{\Psi_N(mx)\xi'_N(x) - m\xi_N(x)\Psi'_N(mx)}, \quad \text{(S4)}$$

where Ψ_N and ξ_N are the Riccati-Bessel functions, Ψ'_N and ξ'_N are the first differentiations, and $x = 2\pi n_m R/\lambda$ and $m = (n + ik)/n_m$, where n is the real part of refractive index of a particle, R the radius of the particle, k the imaginary part of the refractive index of the particle (MoS_2), λ excitation wavelength, and n_m the refractive index of the medium around the particle. We used refractive indices of MoS_2 at 632.8 nm (n = 5.22, k = 1.08) from ref. 4 and n_m = 1.33 of methanol. In the main manuscript, the calculations use not only the dipole term but also the quadrupole term for bulk MoS_2 (i.e., N = 1 and 2).

References:

1 M. Cañamares, C. Chenal, R. Birke, and J. Lombardi, *J Phys Chem C.*, 2008, **112**, 20295–20300.

2 Y. Liu, P. Stradins, and S.-H. Wei, *Sci Adv.*, 2016, **2**, e1600069.

3 J. Kang, S. Tongay, J. Zhou, J. Li, and J. Wu, *Appl Phys Lett.*, 2013, **102**, 012111.

4 G. Rubio-Bollinger, R. Guerrero, D. Lara, J. Quereda, L. Vaquero-Garzon, N. Agraït, R. Bratschitsch, and A. Castellanos-Gomez, *Electronics*, 2015, **4**, 847–856.

5 (a) Bohren, C. F. Huffman, D. R. Absorption and Scattering of Light by Small Particles; Wiley-VCH: Weinheim, 2004. (b) K. Saitow, T. Yamamura, and T. Minami, *J Phys Chem C.*, 2008, **112**, 18340–18349. (c) M.Schmid , P. Andrae and P. Manley, *Nanoscale Research Letter*, 2014, **9**, 50.